ISSN 0022-4766, Journal of Structural Chemistry, 2019, Vol. 60, No. 12, pp. 2001-2008. © Pleiades Publishing, Ltd., 2019.
Russian Text © The Author(s), 2019, published in Zhurnal Strukturnoi Khimii, 2019, Vol. 60, No. 12, pp. 2089-2096.

DETERMINATION OF THE DIAMETER DISTRIBUTION FUNCTION OF SINGLE-WALL CARBON NANOTUBES BY THE X-RAY DIFFRACTION DATA

I. N. Salamatov[1]*, D. A. Yatsenko[1,2], and A. A. Khasin[3]**

A method to construct an atomic model of bundles consisting of single-wall carbon nanotubes with different diameters is proposed. It takes into account the appearing distortions of the close packing and helps calculate X-ray diffraction patterns by the Debye scattering equation. This method is demonstrated on a Tuball^{TM}(OCSiAl) sample. Its application provides information on the diameter distribution function of nanotubes.

DOI: 10.1134/S0022476619120175

Keywords: X-ray diffraction, carbon nanotubes, SWCNT bundles, close packing, Debye scattering equation.

INTRODUCTION

Single-wall carbon nanotubes (SWCNTs) have unique physical and chemical properties. A high Young's modulus of about 0.9 TPa enables the creation of novel high-strength nanocomposite materials [1-3]. Even their low concentrations in the total mass of the material (from 0.01%) confer electrical conductivity and improve the physicomechanical properties of plastics and elastomers [4, 5]. Thus, having added 1% SWCNT, L. Sun and others increased the Young's modulus and the strength limit of the SWCNT/epoxy composite by 27% and 17% respectively [6]. Apart from the unique mechanical properties, SWCNTs also possess excellent thermal and electrical properties. They are thermostable up to 2800°C in vacuum [7], and their coefficient of thermal conductivity is approximately 2000 W/mC [8]. SWCNTs with chirality (n, m) at $n = m$ or difference $n - m$ multiple of 3 exhibit metallic properties, with the characteristic specific electrical resistivity of SWCNTs being below 10^{-4} Ohm·cm, and the current density of $6 \cdot 10^6$ A·cm^{-2}, which more than 1000 times exceeds the maximum current density in copper, does not cause their destruction [9]. The mentioned properties ensure the great potential application of SWCNTs in electronics, allow the development of nanotransistors, nanowires, and transparent conductive surfaces. Moreover, the conductivity of semiconductor SWCNTs strongly depends on adsorbed particles, owing to which, SWCNT can detect with a high sensitivity gases, such as NH_3, NO_2, CO, which enables their use as gas sensors [10-12]. All these facts makes SWCNTs highly promising as technological materials. Structure data are required for their practical application, controlled synthesis, the study of properties.

[1]Novosibirsk State University, Novosibirsk, Russia; *salamatov-in@mail.ru. [2]Boreskov Institute of Catalysis, Siberian Branch, Russian Academy of Sciences, Novosibirsk, Russia. [3]International Scientific Center for Thermophysics and Power Engineering (OCSiAl Group), Novosibirsk, Russia; **khasin.aa@ocsial.com. Original article submitted Received April 14, 2019; revised May 21, 2019; accepted June 10, 2019.

SWCNTs are known to represent a folded graphene sheet, and as a result of van der Waals forces, nanotubes are attracted to each other and self-organized, forming bundles with a two-dimensional close packing [13, 14]. The structure of separate SWCNTs has been well studied, however, the majority of industrial samples have a sufficiently wide tube diameter distribution. Since the properties of nanotubes depend on their structural characteristics, the information on the SWCNT diameter distribution is extremely useful for their further application. Thus, it is still of interest to develop procedures to characterize real samples.

To estimate tube diameters the following research techniques have been widely applied: scanning and tunnel microscopy, transmission electron microscopy (TEM), optical absorption and Raman spectroscopy, X-ray diffraction, and others. Thus, for instance, from the breathing mode of the Raman spectrum of SWCNTs it is possible to find their average diameter [15, 16] while the information on the local bundle size distribution is obtained, as a rule, from TEM data. At the same time, X-ray diffraction is one of the most popular methods to study the structure of materials because this technique is non-destructive, practically does not require a special sample preparation, and provides the possibility of performing the integral analysis and obtaining statistically correct data on the structure of materials under study.

The range of medium and far angles of the diffraction pattern contains information on the internal structure of SWCNTs, metallic catalyst, and other possible impurities. In this work, we focused on the range of small angles (up to 10° 2θ CuK_α) where the scattering from the two-dimensional SWCNT close packing is observed. For SWCNT bundles the Miller indices *hkl* corresponding to crystallographic directions are written in the *hk* format because for two-dimensional systems the *l* index is always zero. Most intense peak 10 observed at ~6° 2θ (d_{10} ~ 1.5 nm) in the diffraction pattern corresponds just to the nanostructure of the bundles. The distance between the tube centers is determined by the crystal lattice parameter. For the ideal packing

$$a = d_{\mathrm{SWCNT}} + d_{t\text{-}t}, \tag{1}$$

where d_{SWCNT} is the diameter of nanotubes; $d_{t\text{-}t}$ is the distance between the cylindrical surfaces formed by centers of atoms of graphene layers of the neighboring tubes. It is usually taken to be 0.32 nm [17].

As a rule, according to TEM data, a wide nanotube diameter and packing defect distribution is observed in SWCNT samples. This causes difficulties in applying standard X-ray crystallographic methods of analysis that are often used to estimate the average particle size. Despite that some authors use the Rietveld method to analyze the diffraction data from SWCNT bundles [18], the most employed approach is the calculation of the entire profile of diffraction patterns of ordered objects.As a model of tubes, most authors use the approximation of infinitely long hollow cylinders with the uniformly distributed scattering density on the surface (cylinder approximation). For them the scattering is the form-factor. This approach allows them to explain many diffraction features and its application is relatively simple. Furthermore, in its frameworks, an approach has been developed to calculate diffraction patterns of models having the SWCNT diameter distribution. The greatest disadvantage of this model is that the distribution is taken into account by summing the diffraction patterns calculated from ideal bundles consisting of identical tubes (the tube diameter varies from one bundle to another). However, the TEM images demonstrate the SWCNT diameter variation just in one bundle (because during the organization of bundles nanotubes do not select identical neighbors) and this leads to packing distortions. In this work, we propose a new, not previously used method to construct atomic models and calculate diffraction patterns of polydisperse SWCNT bundles consisting of nanotubes with different diameters (the tube diameter varies in each bundle).

CALCULATION OF DIFFRACTION PATTERNS

To calculate the diffraction patterns of polydisperse SWCNT bundles we used the method based on the Debye scattering equation (DSE) [28, 29], which allows the calculation of any ensemble of atoms, including nanostructured object, that reflects the relationship between the X-ray scattering intensity and interatomic distances. The diffraction patterns of SWCNTs have been calculated previously with the use of DSE [30, 31], however, the authors constructed the models of only

separate tube to analyze the internal SWCNT structure and determine their chirality in model samples consisting of almost identical SWCNTs.

For complicated systems the main difficulty in applying DSE is the derivation of the full atomic model. To this end, a software was written in C++ that enables the derivation and calculation of diffraction patterns of single SWCNTs, mono- and polydisperse SWCNT bundles by the analytical distribution function.

The atomic model of a polydisperse bundle is constructed iteratively. A new nanotube with an arbitrary radius R_t from the preset distribution function is generated at each step, with its chirality being selected randomly. Then this tube is added to the bundle. All pairs of the neighboring tubes with radii R_i and R_j are sorted out in the bundle, and for each of them there can be two positions of the possible new tube in the intersection points of circles with radii $R_1 = R_i + R_t + d_{t\text{-}t}$ and $R_2 = R_j + R_t + d_{t\text{-}t}$ (Fig. 1). Finally, the allowed position of the tube that is nearest to the bundle center of mass is selected.

In this model, each SWCNT has a graphene structure with regard to chirality. Since in the construction of the atomic model the diameter of each nanotube in the bundle is a random value, then different bundles are obtained when the same distribution function is used. Therefore, an ensemble of bundles is modeled and their diffraction patterns are averaged. It is found that for the calculations of diffraction patterns to be reproducible the ensemble size must be no less than 50 bundles.

EXPERIMENTAL

Diffraction experiments were conducted in the Laboratory of Structural Research Methods, Boreskov Institute of Catalysis, Siberian Branch, Russian Academy of Sciences. Diffraction patterns were measured on an X′TRA powder diffractometer (Thermo, Switzerland, vertical θ/θ geometry goniometer, Bragg–Brentano focusing, point semiconductor detector). The radiation source is an X-ray tube with a copper anode and an average radiation wavelength CuK_α = 0.15418 nm. The generator current was 40 mA, voltage 35 kV (power 1.4 kW). The measurement step was 0.05° 2θ and the point acquisition time was 6 s. The measurement was performed in a single crystal cuvette, not contributing to the diffraction data.

High-resolution TEM data were obtained on a JEM-2010 (JEOL, Japan) electron microscope with an accelerating voltage of 200 kV and a resolution of 0.14 nm.

The samples of chemically purified Tuball^{TM} 01RW03 SWCNTs (422 batch) were provided by the OCSiAl Group. According to the certified data of the company, the samples contain 99 wt.% of carbon and less than 1 wt.% of metallic impurities and represent mainly (more than 95 wt.%) SWCNTs. The specific surface found by BET is 1130 m^2/g. The Raman spectra (λ = 532 nm, Fig. 2) contain a set of lines characteristic of SWCNTs with the ratio G/D = 103 and the maximum vibrational energy of breathing modes (RBM) of 179 cm^{-1}.

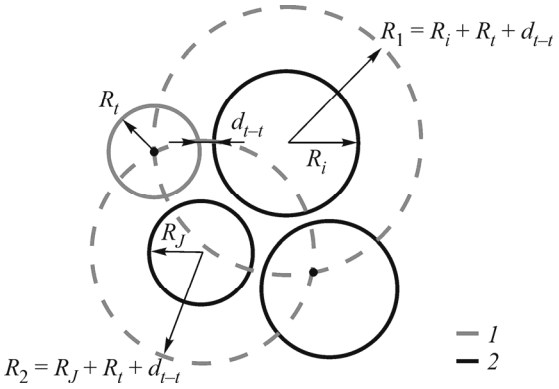

Fig. 1. Scheme of determining the position of a new tube (*1*) in the bundle based on the pair of existing tubes (*2*).

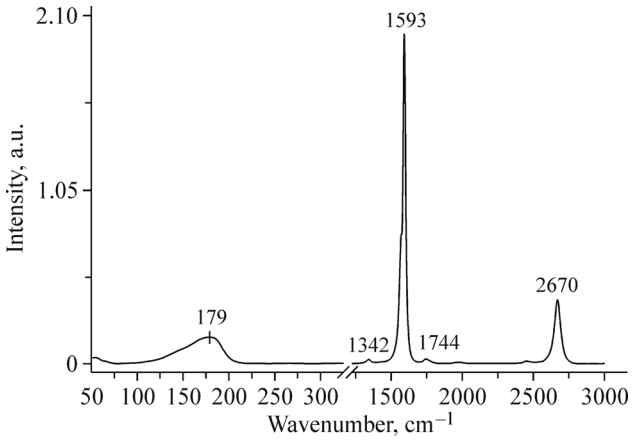

Fig. 2. Raman spectrum of the studied sample with $\lambda = 532$ nm (data of the OCSiAl group).

Taking into account the ratio between the RBM energy and their diameter [32]

$$w(\text{cm}^{-1}) = 234/d(\text{nm}) + 10, \quad (2)$$

it is possible to evaluate that the diameter of SWCNTs in the Tuball^{TM} sample is distributed in the range from 1.2 nm to 2.0 nm with the distribution maximum of about 1.4 nm.

RESULTS

Fig. 3 depicts the experimental diffraction pattern of the studied sample. It exhibits peak 002 at 26.5° 2θ from the coarse graphite impurity and a halo at 22.7° that seems to correspond to a fine graphite-like impurity [33, 34]. Broad maxima at 43° 2θ ($d_{100} \approx 0.21$ nm) and 80° 2θ ($d_{110} \approx 0.12$ nm) are due to the scattering from the SWCNT graphene structure and correspond to diffraction from graphite *hk*0 planes with interplanar distances $d_{100} = 0.214$ nm and $d_{110} = 0.124$ nm [35]. In this work, we focus our attention on most intense peak 10 corresponding to the packing of SWCNTs into bundles.

Within the calculation procedure proposed, it is necessary to determine the diameter of SWCNT bundles. By means of the cylinder model, S. Rols et al. have previously shown that the size effect substantially influences the diffraction pattern only of bundles with the cross-section below 20 nm [17]. Thus, in the calculation of diffraction patterns of bundles with large diameter, their diameter distribution may be neglected. Our simulation of the diffraction patterns of monodisperse SWCNT bundles consisting of tubes with a diameter of 1.5 nm and a length of 2.5 nm confirmed the conclusions of S. Rols and

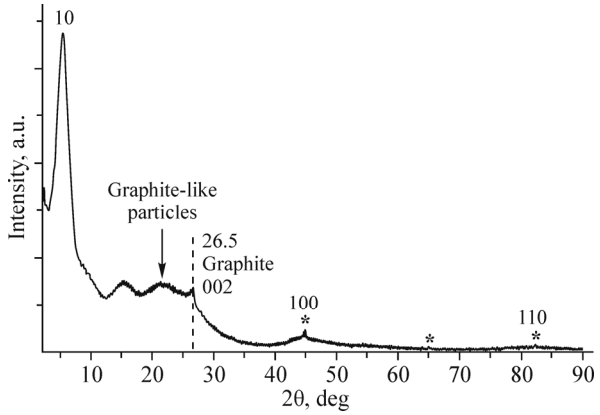

Fig. 3. Experimental diffraction pattern of the studied sample. Peaks of coarse and fine graphite-like impurities, an iron catalyst (*), whose mass concentration in the sample is below 1%, are marked.

coauthors: when the number of tubes exceeds 100 in the bundle (which corresponds to the bundle diameter of about 20 nm) the width of peak 10 hardly changes. According to the TEM images, cross-sections of the bundles amount to 20-50 nm (Fig. 4). Therefore, the characteristic sizes of the bundles in the samples are so that the cross-section distribution effect is negligibly small, and to reduce the calculations a minimum value of 20 nm can be fixed.

Fig. 5 illustrates the calculated diffraction patterns of SWCNT bundles. The model uses the normal distribution with an average value of 1.5 nm and a standard deviation of 0.25 nm. It is seen that when the distribution is taken into account, in both models the diffraction maxima are broadened up to blurring of all peaks (except 10), however, its shape is different in the two models.

By varying the average diameter and the standard deviation of the normal SWCNT diameter distribution so that the calculated diffraction pattern would best describe the experiment, we failed to obtain good results. Having achieved good correspondence with the right shoulder of peak 10, we could not describe it from the side of small angles. This indicates the

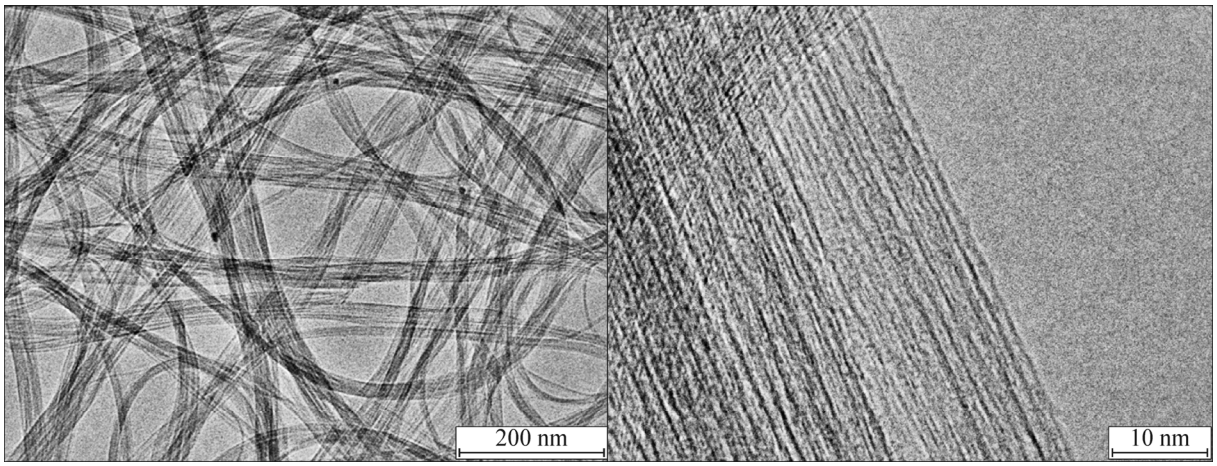

Fig. 4. TEM images of the Tuball^{TM} sample (422 batch) (data of the OCSiAl Group).

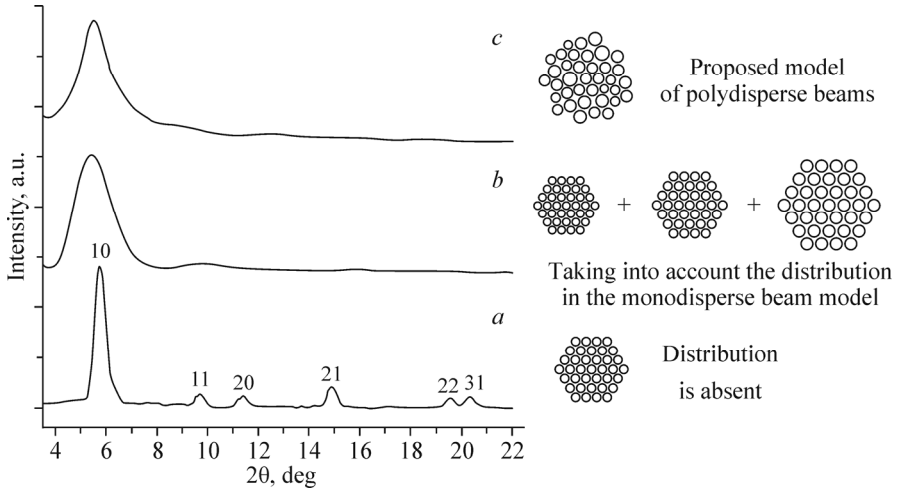

Fig. 5. Calculated diffraction patterns of SWCNT bundles: without the SWCNT diameter distribution (*a*); with the distribution in the approximation of monodisperse bundles (*b*); with the distribution in the model of polydisperse bundles (*c*). The model used is schematically presented on the right (in fact, bundles of 100 tubes were used in the calculation).

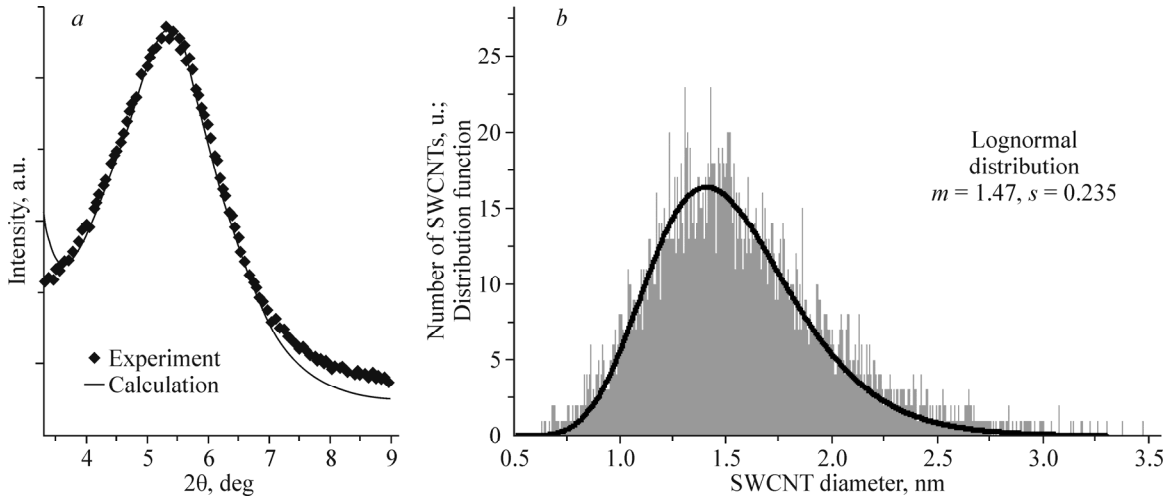

Fig. 6. Region of peak 10 in the experimental and calculated diffraction patterns of polydisperse SWCNT bundles (*a*). The lognormal SWCNT diameter distribution function with parameters $m = 1.47$, $s = 0.235$ (*b*) which corresponds to the calculations.

asymmetry of the distribution function and the occurrence of a tail towards large diameters. The lognormal distribution function corresponds to this distribution

$$f(d) = \frac{1}{sd\sqrt{2\pi}} e^{-\frac{(\ln(d)-\ln(m))^2}{2s^2}}, \quad (3)$$

where m and s are the refined parameters. The fact that the nanotube diameter obeys the lognormal distribution function is also supported in the literature by works using TEM studies [36-38]. As a result of fitting, the lognormal distribution parameters are optimized for the more accurate description of the peak 10 profile for the studied SWCNT sample (Fig. 6).

CONCLUSIONS

We have developed the approach to calculate the diffraction patterns of SWCNTs, which is based on DSE. We also propose a new model to construct bundles consisting of nanotubes with different diameters, which makes it possible to take into account the nanotube diameter distribution directly in the atomic structure and the non-ideal packing. It is found that it is impossible to describe the experimental data in the approximation of the normal distribution and the approximation of the lognormal SWCNT diameter distribution function is needed. The procedure is proposed to obtain data on the SWCNT diameter distribution function and it is exemplified by a real Tuball™ SWCNT sample (OCSiAl).

ACKNOWLEDGMENTS

SWCNT samples were provided by the OCSiAl Group.

FUNDING

The work was performed within the State Contract of the Boreskov Institute of Catalysis, Siberian Branch, Russian Academy of Sciences (project AAAA-A17-117041710079-8).

CONFLICT OF INTERESTS

The authors declare that they have no conflict of interests.

REFERENCES

1. P. M. Agrawal, B. S. Sudalayandi, L. M. Raff, and R. Komanduri. *Comput. Mater. Sci.*, **2006**, *38*, 271.
2. M. Meo and M. Rossi. *Compos. Sci. Technol.*, **2006**, *66*, 1597.
3. B. W. Xing, Z. C. Chun, and C. W. Zhao. *Physica*, **2004**, *352*, 156.
4. Q.-P. Feng, X.-J. Shen, J.-P. Yang, S.-Y. Fu, Y.-W. Mai, and K. Friedrich. *Polymer*, **2011**, *52*, 6037.
5. X. Xu, A.J. Uddin, K. Aoki, Y. Gotoh, T. Saito, and M. Yumura. *Carbon*, **2010**, *48*, 1977.
6. L. Sun, G. L. Warren, J. Y. O′Reillya, W. N. Everett, S. M. Lee, D. Davis, D. Lagoudas, and H.-J. Suea. *Carbon*, **2008**, *46*, 320.
7. P. G. Collins and P. Avouris. *Sci. Am.*, **2000**, 62.
8. M. Fujii, X. Zhang, H. Xie, H. Ago, K. Takahashi, T. Ikuta, H. Abe, and T. Shimizu. *Phys. Rev. Lett.*, **2005**, 95.
9. T. W. Ebbesen, H. J. Lezec, H. Hiura, J. W. Bennett, H. F. Ghaemi, and T. Thio. *Nature*, **1996**, *382*, 54.
10. S. Chopra, A. Pham, J. Gaillard, A. Parker, and A. M. Rao. *Appl. Phys. Lett.*, **2002**, *80*, 4632.
11. L. Valentini, I. Armentano, J. M. Kenny, C. Cantalini, and L. Lozzi. *Appl. Phys. Lett.*, **2003**, *82*, 961.
12. J. A. Talla. *Physica*, **2012**, *407*, 966.
13. M. S. Dresselhaus, G. Dresselhaus, and R. Saito. *Carbon*, **1995**, *33*, 883.
14. A. Thess, R. Lee, P. Nikolaev, and H. Dai. *Science*, **1996**, *274*, 483.
15. T. Belin and F. Epron. *Mater. Sci. Engin.*, **2005**, *119*, 105.
16. L. Alvarez, A. Righi, T. Guillard, S. Rols, E. Anglaret, D. Laplaze, and J.-L. Sauvajol. *Chem. Phys. Lett.*, **2000**, *316*, 186.
17. S. Rols, R. Almairac, L. Henrard, E. Anglaret, and J.-L. Sauvajol. *Eur. Phys. J.*, **1998**, *10*, 263.
18. H. Kadowaki, A. Nishiyama, K. Matsuda, Y. Maniwa, S. Suzuki, Y. Achiba, and H. Kataura. *J. Phys. Soc. Jpn.*, **2005**, *74*, 2990.
19. A. G. Rinzler, J. Liu, H. Dai, P. Nikolaev, C. B. Huffman, F. J. Rodríguez-Macías, P. J. Boul, A. H. Lu, D. Heymann, D. T. Colbert, R. S. Lee, J. E. Fischer, A. M. Rao, P. C. Eklund, and R. E. Smalley. *Appl. Phys.*, **1998**, *67*, 29.
20. M. Abe, H. Kataura, H. Kira, T. Kodama, S. Suzuki, Y. Achiba, K. Kato, M. Takata, A. Fujiwara, K. Matsuda, and Y. Maniwa. *Phys. Rev.*, **2003**, *68*, 041405.
21. Y. Maniwa, Y. Kumazawa, Y. Saito, H. Tou, H. Kataura, Hiroyoshi Ishii, S. Suzuki, Y. Aachiba, A. Fujiwara, and H. Suematsu. *Jpn. J. Appl. Phys.*, **1999**, *38*, 668.
22. Y. Maniwa, R. Fujiwara, H. Kira, H. Tou, H. Kataura, S. Suzuki, Y. Achiba, E. Nishibori, M. Takata, M. Sakata, A. Fujiwara, and H. Suematsu. *Phys. Rev.*, **2001**, 64.
23. G. Liu, Y. Zhao, K. Deng, Z. Liu, W. Chu, J. Chen, Y. Yang, K. Zheng, H. Huang, W. Ma, L. Song, H. Yang, C. Gu, G. Rao, C. Wang, S. Xie, and L. Sun. *Nano Lett.*, **2008**, *8*, 1071.
24. I. Hinkov, J. Grand, M.L. de la Chapelle, S. Farhata, C. D. Scott, P. Nikolaev, G. B. Tech, V. Pichot, P. Launois, J. Y. Mevellec, and S. Lefrant. *J. Appl. Phys.*, **2004**, *96*, 2029.
25. N. Bendiab, R. Almairac, S. Rols, R. Aznar, J.-L. Sauvajol, and I. Mirebeau. *Phys. Rev.*, **2004**, 69.
26. A. Giannasi, M. Celli, J. L. Sauvajol, M. Zoppi, and D. T. Bowron. *Physica*, **2004**, *350*, 1027.
27. R. M. Allaf, I. V. Rivero, S. S. Spearman, and L. J. Hope-Weeks. *Mater. Character.*, **2011**, *62*, 857.
28. S. V. Tsybulya and D. A. Yatsenko. *J. Struct. Chem.*, **2012**, *53*, 150.
29. P. Debye. *Ann. Physik*, **1915**, *351*, 809.
30. R. Mitsuyama, S. Tadera, H. Kyakuno, R. Suzuki, H. Ishii, Y. Nakai, Y. Miyata, K. Yanagi, H. Kataura, and Y. Maniwa. *Carbon*, **2014**, *75*, 299.
31. B. Emmanuel, S. Thomas, G. Raghuvaran, and D. Sherwood. *J. Alloys Compd.*, **2009**, *479*, 484.
32. M. S. Dresselhaus, G. Dresselhaus, R. Saito, and A. Jorio. *Phys. Rep.*, **2005**, *409*, 47.

33. J. B. Aladekomo and R. H. Bragg. *Carbon*, **1990**, *28*, 897.
34. E. A. Belenkov. *Inorg. Mater.*, **2001**, *37*, 928.
35. I. Sanc. Foreing Trade Corporation. Panska, Czechoslovakia, ICDD Grant-in-Aid, **1990**.
36. M. He, Y. Magnin, H. Jiang, H. Amara, E. I. Kauppinen, A. Loiseau, and C. Bichara. *Nanoscale*, **2018**, *10*, 6744.
37. M. Li, X. Liu, X. Zhao, F. Yang, X. Wang, and Y. Li. *Top. Curr. Chem.*, **2017**, *375*, 29.
38. J. S. Barnard, C. Paukner, and K. K. Koziol. *Nanoscale*, **2016**, *8*, 17262.